Eur Biophys J (1994) 23:167–176

European Biophysics Journal

A spectroscopic characterization of a monomeric analog of copper, zinc superoxide dismutase

Ivano Bertini [1], Mario Piccioli [1], Maria Silvia Viezzoli [1], Choi Ying Chiu [2], Guy T. Mullenbach [2]*

[1] Department of Chemistry, University of Florence, I-50121 Florence, Italy
[2] Chiron Corporation, Emeryville, CA 94608, USA

Received: 28 February 1994 / Accepted: 12 May 1994

Abstract. A mutated protein of human $Cu(II)_2Zn(II)_2$ SOD in which residues Phe50 and Gly51 at the dimer interface were substituted by Glu's, thus producing a monomeric species, has been characterized by electronic absorption spectroscopy, EPR, relaxivity and ^1H NMR techniques. Such substitutions and/or accompanying remodeling and exposure of the dimer interface to solvent, alter the geometry of the active site: increases in the axiality of the copper chromophore and the Cu-OH_2 distance have been observed. The affinity of both metal binding sites for Co(II) is also altered. The observed NMR parameters of the Co(II) substituted derivative have been interpreted as a function of the decrease of rotational correlation time as a consequence of the lower molecular weight of the mutated protein. Sharper NMR signals are also obtained for the reduced diamagnetic enzyme. Results are consistent with an active site structure similar to that observed for the dimeric analog Thr137Ile characterized elsewhere. An observed proportional decrease in enzymatic activity and affinity for the N_3-anion suggests the importance of electrostatic forces during substrate docking and catalysis.

Key words: Cu, Zn, Superoxide Dismutase – ^1H NMR – Monomeric analog

Introduction

Superoxide Dismutase (SOD or WT-$Cu(II)_2Zn(II)_2$-SOD) is a homo-dimeric enzyme of 16,000 MW per subunit, containing a copper and zinc ion per subunit whose physiological role is the dismutation of the superoxide radical to hydrogen peroxide and molecular oxygen (Fridovich 1974; Valentine and Pantoliano 1982; Tainer et al. 1982; Fridovich 1987; Banci et al. 1990a). The enzymatic reaction occurs through a two step mechanism involving the reduction of copper(II) to copper(I) by a first moiety of superoxide and the reoxidation of copper(I) with a second moiety. The copper(II) ion is located at the bottom of a cavity about 1 nm deep (Tainer et al. 1982). The role of aminoacids constituting the catalytic cavity of SOD has been extensively investigated through site directed mutagenesis techniques. Various mutated proteins have been characterized using several spectroscopic techniques (Beyer et al. 1987; Banci et al. 1988, 1990b, 1991a; Bertini et al. 1989) and the functional roles of various residues in catalysis have been deduced accordingly. For example, Arg143 and Thr 137 face each other at the entrance to the active site cavity where the cationic Arg143 is apparently positioned to guide the superoxide anion to the active site. Accordingly, replacement with neutral or negative residues produces dramatic decreases in enzymatic activity (Beyer et al. 1987; Banci et al. 1988). Furthermore, it has been observed that Thr137 is involved in hydrogen-bonding with Glu133 and Lys136 and contributes to the hydrophilicity of the cavity (Bertini et al. 1989; Banci et al. 1990b). Indeed, the substitution of Thr with a hydrophobic residue such as Ile causes a water molecule to be expelled (Bertini et al. 1989) which is otherwise weakly coordinated to copper (Banci et al. 1990a). The copper and zinc ions are bridged by an imidazole group of a histidine in each subunit. Copper(II) is also coordinated to three other histidines and semi-coordinated to a water molecule in a distorted square pyramidal geometry. Zinc(II) is also bound to two other histidines and to an aspartate residue in a distorted tetrahedral coordination geometry. A schematic drawing of the active site is shown in Fig. 1. Both metal binding sites can also accommodate other metal ions [e.g. cobalt(II) and nickel(II)]. The protein maintains its enzymatic activity, however, only in those derivatives where copper(II) occupies its native site (Valentine and Pantoliano 1982). Cobalt(II) has proven to be a useful spectroscopic probe because it gives rise to well shaped and informative electronic spectra (Bertini et al. 1986). Furthermore, high spin cobalt(II) can be used to detect hyperfine-shifted NMR signals of

* *Present address:* Lynx Therapeutics, Foster City, CA 94404, USA
Correspondence to: I. Bertini

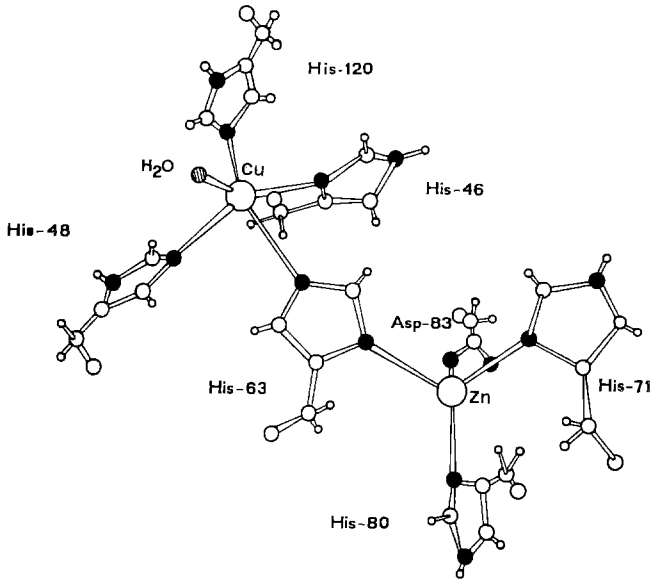

Fig. 1. Schematic drawing of the metal sites of human WT-$Cu(II)_2Zn(II)_2SOD$

ligands coordinated to the paramagnetic Co(II) ion (Bertini and Luchinat 1986). The native wild type oxidized enzyme (WT-$Cu(II)_2Zn(II)_2$-SOD) is not suitable for NMR investigation of structure around copper(II) since signals are too broad to detect. Substitution of Zn(II) with Co(II), however, has allowed ^1H NMR characterization of the Cu(II) site (Bertini et al. 1985a; Banci et al. 1987, 1989a). Indeed, magnetic coupling between cobalt(II) and copper(II) has permitted the observation as well as the assignment of those ^1H NMR signals arising from ligand-associated protons.

The dimeric nature of the protein originates from hydrophobic interactions at the interface. Specifically residues Phe50 and Gly51 provide intersubunit hydrophobic and hydrogen bonding interactions respectively, that stabilize quaternary structure. Since SOD can be expressed efficiently in yeast (Beyer et al. 1987) and in *E. coli* (Banci et al. 1991a; Getzoff et al. 1992), a series of analogs were prepared where hydrophobic residues were substituted with charged residues (Mullenbach et al., unpublished results).

We report here a biophysical characterization of a mutated protein in which Phe50 and Gly51 were both substituted with Glu (i.e. M-Cu(II)Zn(II)SOD, hereafter). The protein is monomeric. The catalytic cavity has been investigated through NMR, EPR and electronic absorption spectroscopy. The spectroscopic parameters have been related to the functional properties. The rationale for substitutions of Phe50 and Gly51, as proposed by John Tainer and Elizabeth Getzoff is discussed in a joint manuscript in preparation (Mullenbach et al., unpublished results).

Material and methods

Preparation of the protein

The M-Cu(II)Zn(II)SOD mutated protein was expressed and isolated from *E. coli* cultures (strain MC1061) using a procedure previously reported (Banci et al. 1991a). The mutated protein was purified by ion exchange chromatography on DEAE Sepharose CL-6B (Pharmacia). The molecular weight of the protein sample was checked through gel filtration experiments using a column packed with Sephadex G75 and equilibrated with 50 mM Tris-HCl, 100 mM NaCl, pH 7.0. In order to obtain a calibration line, different mixtures of standards (myoglobin, carbonic anhydrase, wild type SOD) were loaded on the column. Transferrin was used in all the mixtures to determine the void volume. Protein concentration was calculated from dry weight for a solution of the mutated protein and an extinction coefficient at 265 nm of 7400 $cm^{-1}\,M^{-1}$ was calculated from the electronic spectrum of this solution in the ultraviolet region. This extinction coefficient was then used to determine protein concentrations of different samples of M-Cu(II)Zn(II)SOD. Atomic absorption analysis was performed on GBC 903 instrument. Activity measurements were performed using the method by Fridovich (McCord and Fridovich 1969).

Metal substitution

The apoprotein was obtained by dialysis against 10 mM EDTA in 50 mM acetate buffer, pH 3.8 (McCord and Fridovich 1969). EDTA was removed by dialysis against 100 mM NaCl in 50 mM acetate buffer, pH 3.8 and then against acetate buffer alone, gradually increasing the pH from 3.8 to 5.5 (Forman et al. 1973). The WT-$E_2Co(II)_2SOD$ (E = empty) and the M-ECo(II)SOD derivatives were obtained by adding a $CoCl_2$ solution to the apoprotein at pH 5.5 (Rotilio et al. 1972a; Fee 1973; Pantoliano et al. 1979). The metal uptake was followed spectrophotometrically up to the complete development of the electronic spectrum. The WT-$Cu(II)_2Co(II)_2SOD$ and M-Cu(II)Co(II)SOD derivatives were obtained by slow addition over 12 h of a stoichiometric amount of a $CuCl_2$ solution with gentle stirring at room temperature. The samples were concentrated by ultrafiltration using an Amicon cell equipped with a 500 Da cut off membrane.

Reduced analogs

The WT-$Cu(I)_2Zn(II)_2$-SOD and the M-Cu(II)Zn(II)-SOD derivatives were prepared by addition of a few crystals of solid sodium dithionite to the solution of the oxidized species (Cass et al. 1977a; Lippard et al. 1987; Bertini et al. 1991a).

Spectroscopic measurements

All spectroscopic measurements with the exception of ^{1}H NMR spectra were performed in unbuffered water solution, pH 5.5. Electronic spectra were recorded on a Cary 17D spectrophotometer. CD spectra were recorded on JASCO 500C instrument. EPR spectra were recorded at room temperature on a Bruker ER200 operating at 9.8 GHz. Water proton NMRD measurements were performed on a Koenig-Brown relaxometer, installed at the University of Florence thanks to an agreement between the latter and the IBM Watson Research Center of Yorktown Heights, New York. All NMR experiments were recorded on a Bruker AMX600 spectrometer at the magnetic field of 14T or on a Bruker MSL200, operating at 4.7T. They were performed at 298 K, on ca. 4 mM samples, 10 mM phosphate buffer. Experiments were performed at pH 5.1 for WT-Cu(I)$_2$Zn(II)$_2$SOD and M-Cu(I)Zn(II)SOD and at pH 7.0 for WT-Cu(II)$_2$Co(II)$_2$-SOD and M-Cu(II)Co(II)SOD. Chemical shift values were obtained by calibrating the H_2O signal at 4.8 ppm from DSS. The NOESY spectra were recorded in aqueous 10% D_2O solution. In the case of WT-Cu(I)$_2$Zn(II)$_2$SOD and M-Cu(I)Zn(II)SOD, the usual (90°-t_1-90°-t_m-90°-AQ) pulse sequence was modified by replacing the observation 90° pulse with a spin-echo pulse sequence and combining a four-step Exorcycle to the usual receiver phase list for recording NOESY spectra (Sklenar and Bax 1987). This allows the suppression of the intense solvent peak without using a presaturation pulse. We have observed that, when a presaturation pulse is applied on the solvent peak, the intensity of the signals of the NH of histidines dramatically decreases. The NOESY spectra on the Cu(II)Co(II) derivatives were recorded by using a standard presaturation pulse. All the NOESY spectra were collected in phase sensitive absorption mode (TPPI) (Marion and Wuthrich 1983). 2K × 512 data points were acquired. Square sine shifted functions were applied to acquired data prior to Fourier transformation. A standard software package provided by Bruker was used for data processing. One-dimensional NOE experiments were recorded at 200 MHz using the previously reported methodology (Banci et al. 1989a; Lecomte et al. 1991). T_1 values were obtained using the inversion recovery methodology (Inubushi and Becker 1983). Titration with sodium azide was performed at 200 MHz essentially as reported elsewhere (Bertini et al. 1985a; Banci et al. 1987).

Results and discussion

The molecular weight of the protein was checked to be 16,000±3,000. The content of copper(II) and zinc(II) measured using atomic absorption analysis has revealed that the copper content is 99% and the zinc content is 100%. The activity of the M-Cu(II)Zn(II)SOD, measured with the method of Fridovich (McCord and Fridovich 1969) and expressed as a function of copper(II) content, was found to be 10±5% of that found for the wild type Cu(II)$_2$Zn(II)$_2$SOD. Since the copper content is

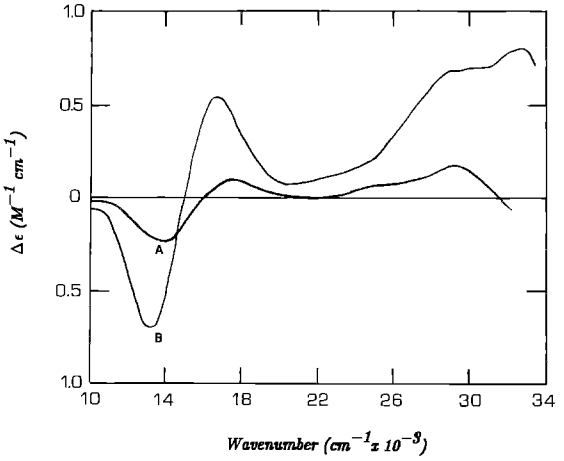

Fig. 2. Circular dichroism spectra of M-Cu(II)Zn(II)SOD **A** and WT-Cu(II)$_2$Zn(II)$_2$SOD **B**. Samples were in unbuffered water, at pH 5.5. $\Delta\varepsilon$ is expressed per mol of copper

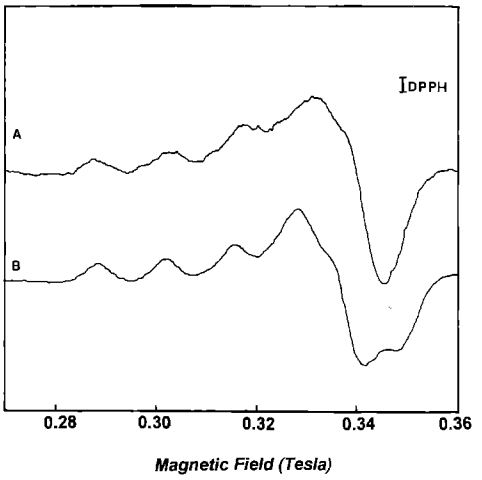

Fig. 3. Room temperature EPR spectra of M-Cu(II)Zn(II)SOD **A** and WT-Cu(II)$_2$Zn(II)$_2$SOD **B**

comparable with the wild type protein and constant with time, we cannot ascribed the decreased activity to alteration in the affinity for copper.

CD and electronic spectra

The electronic spectrum of M-Cu(II)Zn(II)SOD is nearly indistinguishable from that of the wild type enzyme (Pantoliano et al. 1982; Banci et al. 1990c). However, the CD spectrum (Fig. 2) shows d-d transitions at 13800 and 17400 cm^{-1} which compare with 13300 and 16700 cm^{-1} in the wild type enzyme, whereas the charge transfer band remain unchanged. Ipsochromic shift of the d-d transitions of copper(II) has been interpreted as a geometric change towards planarity of the coordinated histidines (Lever 1984; Banci et al. 1990c, d).

EPR spectra

EPR spectra of wild type SOD and the monomeric analog are shown in Fig. 3. The spectrum of M-

Cu(II)Zn(II)SOD indicates a rather axial geometry whereas, in WT-$Cu(II)_2Zn(II)_2SOD$ a rhombic component is apparent as extensively discussed (Rotilio et al. 1972b; Bertini and Scozzafava 1981). The $g_\perp$ value of 2.26 is the same as for the wild type enzyme; the $g_\parallel$ value is 2.06 which compares with 2.09 in the wild type (the latter value represents the reading of the $g_x + g_y$ feature in the first derivative spectrum) (Banci et al. 1990a, 1991b). The $A_\parallel$ value is 151×10^{-4} cm^{-1}, whereas it is 138×10^{-4} cm^{-1} in the wild type. Such an increase in $A_\parallel$ as well as an axial geometry indicated by the spectrum has been observed in the anion derivatives of the wild type enzyme (Banci et al. 1990d) and in some mutated proteins (Banci et al. 1990d).

Relaxivity measurements

The water ^1H NMRD profiles (Bertini et al. 1985b; Koenig and Brown 1987; Koenig and Brown 1990) of M-Cu(II)Zn(II)SOD mutated protein and WT-$Cu(II)_2Zn(II)_2SOD$, recorded between 0.01 and 50 MHz (Fig. 4) have similar shapes, indicating that the correlation time τ_c is unchanged in the mutated protein. The correlation time is given by the electronic relaxation time (Bertini and Luchinat 1986). However the monomer has 20% lower relaxivity than the wild type, which may be ascribed to a slightly longer $Cu-OH_2$ distance. In the WT-$Cu(II)_2Zn(II)_2SOD$ the Cu–O distance has been estimated to be around 0.27 nm (Tainer et al. 1982), a value in accordance with EXAFS data (Blackburn et al. 1984). A 20% decrease in T_1^{-1} corresponds to about a 5% increase in the Cu–O distance.

^1H NMR spectroscopy

Cobalt derivative. Addition of Co(II) ion to the monomeric metal-deprived M-SOD in a ratio metal : protein of 1 : 1 gives rise to a derivative whose ^1H NMR spectrum resembles that of the dimeric WT-$Co(II)_2Co(II)_2SOD$ (Banci et al. 1986) (Fig. 5). We propose that the affinity for metal ions of the two metal sites in the monomeric analog is altered and that Co(II) also binds at the copper site even at pH 5.5 (whereas the wild type enzyme at pH 5.5 binds Co(II) only in the zinc site) (Valentine and Pantoliano 1982). This proposal is in agreement with the spectrophotometric titration of the apo M-SOD with Co(II) (data not shown). From the electronic spectrum we calculate an average maximum extinction coefficient of 300 M^{-1} cm^{-1} (the value is related to the Co(II) concentration); this value is lower than the value typical of WT-$E_2Co(II)_2SOD$ (400 M^{-1} cm^{-1}) and could be explained by taking into account a mixture of Co(II) in a tetrahedral site (the zinc site) and in a five-coordinated site (the copper site).

Copper–Cobalt derivative. Figure 6 compares the ^1H NMR spectra of WT-$Cu(II)_2Co(II)_2SOD$ and M-Cu(II)Co(II)SOD at 600 MHz. The latter was obtained by adding a stoichiometric amount of copper(II) to M-ECo(II)SOD. The NMR spectrum shows that copper(II)

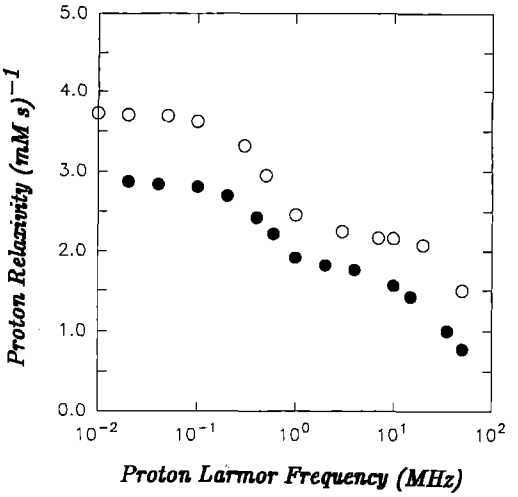

Fig. 4. Water proton NMRD profiles at 298 K, of WT-$Cu(II)_2Zn(II)_2SOD$ (○) and M-Cu(II)Zn(II)SOD (●). Samples were in 10 mM Hepes, pH 7.5. The values have been subtracted of the water and the diamagnetic protein contribution and normalized to 1 mM copper concentration according to the standard procedure of relaxivity data treatment

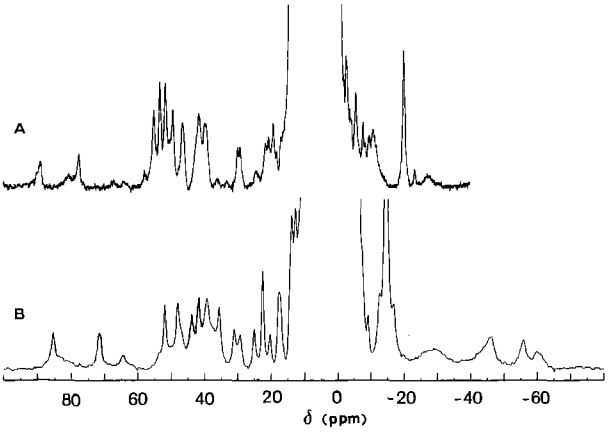

Fig. 5. ^1H NMR spectrum of M-ECo(II)SOD **A**, recorded at 200 MHz in H_2O solutions at pH 5.5. For comparison purposes the spectrum of bovine WT-$Co(II)_2Co(II)_2SOD$ **B**, recorded at 90 MHz, is also shown

binds at the copper center in a quantitative fashion. The assignment follows that already reported for WT-$Cu(II)_2Co(II)_2SOD$. It is apparent that signal linewidths are decreased by about a factor of two for the monomer. This is due to the decrease of the Curie relaxation contribution (Bertini and Luchinat 1986). The contribution to T_2^{-1} (transverse relaxation rate) provided by this mechanism is given by:

$$T_{2M}^{-1} = \frac{1}{5}\left(\frac{\mu_0}{4\pi}\right)^2 \frac{\omega_I^2 g_e^4 \mu_B^4 (S(S+1))^2}{(3kT)^2} \cdot r^{-6}\left(4\tau_r + \frac{3\tau_r}{1+\omega_I^2\tau_r^2}\right)$$

where τ_r is the rotational correlation time, ω_I is the proton Larmoer frequency of the proton, r is the metal to proton distance and the other symbols have their usual meanings.

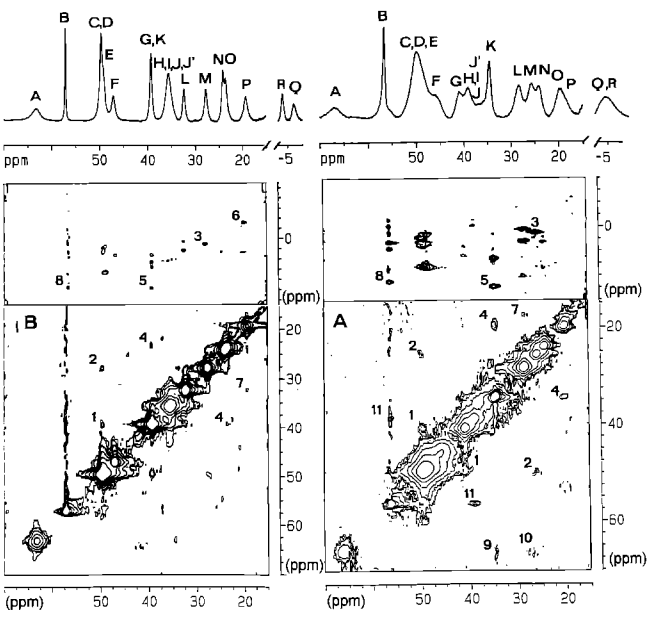

Fig. 6. 600 MHz ^{1}H NMR NOESY spectra of **A** WT-Cu(II)$_2$ Co(II)$_2$SOD and **B** M-Cu(II)Co(II)SOD. The monodimensional spectra of the two derivatives are also reported. Shaded signals disappear in D_2O. Cross peaks are numbered as follows: 1 (C-G), 2 (C-M), 3 (M-CH_3 Ala140), 4 (K-O), 5 (K-His48 Hβ_2), 6 (P-R), 7 (L-P), 8 (B-His120 Hβ_2), 9 (A-K), 10 (A-L), 11 (B-H). Cross peaks 9 to 11 are observed in the dimer derivative; cross peak 6 is observed only in the monomer derivative. Conditions: mixing time 4 ms, relaxation delay 150 ms

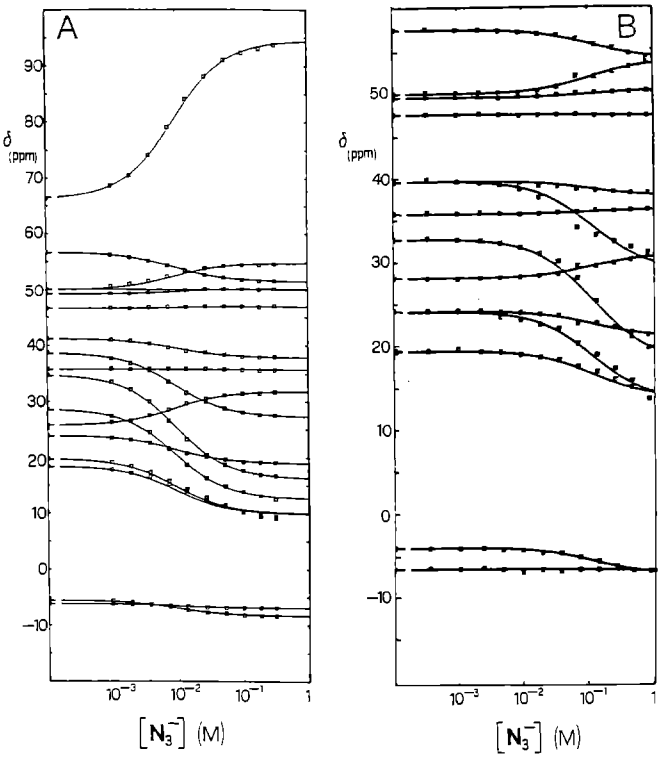

Fig. 7. Chemical shifts of the ^{1}H NMR hyperfine shifted signals of WT-Cu(II)$_2$Co(II)$_2$SOD **A** and M-Cu(II)Co(II)SOD **B** as a function of azide concentration. Experiments were performed at 200 MHz, in H_2O solutions, pH 5.5

At 600 MHz, the Curie relaxation mechanism is expected to be the dominant contribution to the T_2^{-1} in the wild type protein. An inspection of the linewidths of the hyperfine shifted signals as a function of the magnetic field (Bertini et al. 1994), indicates that the contribution to T_2^{-1} due to Curie relaxation mechanism at 600 MHz ranges, in the case of the native dimeric protein, from 70% to 90%, depending on the signal. Therefore, since τ_r is linearly dependent on the molecular size, the Curie contribution to T_2^{-1} is expected to decrease by a factor of two for M-SOD, if the investigated derivative is really a monomeric analog of WT-Cu(II)$_2$Co(II)$_2$SOD. The NMR data provide a nice example of the relevance of the Curie relaxation mechanism in macromolecules at high field and further substantiate the absence of quaternary structure of this analog. The ^{1}H NMR spectrum of copper-cobalt SOD is therefore a very effective tool for monitoring the monomeric nature of Phe50Glu, Gly51Glu mutated protein (M-SOD). Moreover, the decrease of signal linewidths enhances resolution and consequently affords added structural information.

Besides changes in signal linewidths, marked changes in chemical shifts are observed in the ^{1}H NMR spectra of M-Cu(II)Co(II)SOD. Because of those spectral changes, a straightforward assignment of the hyperfine shifted signals by comparison of the WT-Cu(II)$_2$Co(II)$_2$SOD and M-Cu(II)Co(II)SOD cannot be performed. Hence, in order to assign the hyperfine shifted signals, NOESY experiments (Fig. 6) and a titration with sodium azide have been performed (Fig. 7). Figure 6 presents NOESY experiments on M-Cu(II)Co(II)SOD (B) and on WT-Cu(II)$_2$Co(II)$_2$SOD (A). In the NOESY spectrum the advantage of narrower lines for the mutated protein is lost by the lower τ_r which decreases cross relaxation and, as a consequence, the intensities of cross peaks (Ernst et al. 1987; Dugad et al. 1990; Banci et al. 1991 c). Several connectivities can be observed among hyperfine shifted signals on the M-Cu(II)Co(II)SOD derivative. The exchangeable signal at 49.7 ppm is connected to two hyperfine shifted signals at 39.3 ppm and 27.7 ppm (cross peaks 1 and 2, respectively). This pattern has been observed in the dimeric WT-Cu(II)$_2$Co(II)$_2$SOD. In such a case it originated exclusively from His46 NHε_2, which has two vicinal protons on the imidazole ring. On this basis signals at 49.7, 39.3 and 27.7 ppm have been assigned to His46 NHε_2, Hδ_2 and Hε_1, respectively. They are labeled C, G and M according to WT-Cu(II)$_2$Co(II)$_2$SOD assignment. Signals G and M can be distinguished by their NOEs in the diamagnetic region. As discussed for the WT-Cu(II)$_2$Co(II)$_2$SOD (Banci et al. 1989 a, 1993) the strong connectivity (cross peak 3) observed between the signal at 27.7 ppm and a signal at about 1.0 ppm allows assignment of the signal at 27.7 ppm to signal M (Banci et al. 1993). In Fig. 6 A the spectrum of WT-Cu(II)$_2$Co(II)$_2$SOD is reported for comparison purposes. Table 1 reports the observed chemical shifts for the two derivatives. In M-Cu(II)Co(II)SOD the chemical shift of signal C differs from the WT-Cu(II)$_2$Co(II)$_2$SOD by less

than 1 ppm, while a more remarkable difference is experienced by signals G and M, i.e. −1.6 and +2.3 ppm, respectively.

Titration experiments of monomer and dimer with azide (Fig. 7) indicate that three hyperfine shifted signals of monomer (one exchangeable and two non exchangeable) undergo dramatic decreases in their chemical shifts. This is similar to what has been observed in the native protein (Bertini et al. 1985a; Banci et al. 1987) and previously interpreted as related to the increase of the Cu–N His48 bond distances when azide binds to the enzyme (Banci et al. 1989a). This allows us to assign the three signals at 39.4, 32.4 and 23.6 ppm, labeled K, L and O, respectively, to His48 imidazole ring protons. The observed connectivity between signals at 39.4 ppm (overlapping signal G) and 23.6 ppm (cross peak 4, Fig. 6) is consistent with the assignment of K and O as two vicinal protons of the same histidine. Because His48 NHδ_1 (signal K) is 0.24 nm and 0.42 nm apart from His48 Hε_1 and His48 Hδ_2, respectively, the observed connectivity between K and O discriminate between signal O and L which can be assigned to His48 Hε_1 and His48 Hδ_2, respectively. We observe an increase in the hyperfine shift of 4.7 ppm for signal K and 4.0 ppm for signal O and L occurs in the M-Cu(II)Co(II)SOD with respect to the WT-Cu(II)$_2$Co(II)$_2$SOD (see Table 1), corresponding to an increase of 21%, 36% and 19%, respectively, in their hyperfine shifts. The upper part of the two-dimensional spectra of Fig. 6 shows the region of connectivities between the hyperfine shifted signals and the diamagnetic (or slightly hyperfine shifted) signals. In both derivatives signal K experiences a strong cross peak at 12.5 ppm with a signal assigned to His48 Hβ_2 (Banci et al. 1993) (cross peak 5, Fig. 6). Hence, no difference in chemical shift is observed on His48 Hβ_2, which is at variance with what is observed for His48 imidazole ring protons.

A signal at 19.3 ppm (signal P) yields a small cross peak with the signal at 32.4 ppm (signal L) (cross peak 7) already assigned as His48 Hδ_2. Comparison with NOE data on the WT-Cu(II)$_2$Co(II)$_2$SOD allows the assignment of signal P at 19.3 ppm to His46 Hβ_1. The cross peak observed between signals at 19.3 ppm and −3.9 ppm (signal R) (cross peak 6, Fig. 6A) allows the observation of both His46 β-CH$_2$ protons (signals P and R, respectively).

At variance with what is observed in WT-Cu(II)$_2$Co(II)$_2$SOD, in which a cross peak is observed between signals B and H (cross peak 11, Fig. 6A), no clear connectivities are observed from signal B (His120 NHδ_1) in the NOESY spectrum of M-Cu(II)Co(II)SOD in the region 70–15 ppm. The assignment of signal B of M-Cu(II)Co(II)SOD to His20 NHδ_1 is straightforward because of its T_1 and T_2 values and because it exchanges in D_2O solution. A one-dimensional NOE experiment (data not shown) has allowed the observation of connectivity between signal B and a signal at about 36 ppm, a region where the monodimensional spectrum indicates the occurrence of four signals. Among these, the signals I, J and J′ are almost unaffected by titration with sodium azide (Fig. 7) and therefore can be assigned to cobalt-coordinated proton resonances. The fourth signal, overlapping with I, J and J′, is assigned to His120 Hε_1 (signal H) because of NOE experiments. In the diamagnetic region, signal B (His120 NHδ_1) is expected from X-ray data (Tainer et al. 1982) to give a strong connectivity with His120 Hβ_2. In WT-Cu(II)$_2$Co(II)$_2$SOD, His120 Hβ_2 has been recently assigned at 11.1 ppm (cross peak 8, Fig. 6A), while in the monomer derivative the same connectivity is observed at 12.2 ppm. Hence, in the latter derivative His120 Hβ_2 is shifted downfield about 1 ppm more with respect to the dimer.

Table 1. Chemical shifts of the hyperfine shifted signals of M-Cu(II)Co(II)SOD, recorded at 298 K, and compared with WT-Cu(II)$_2$Co(II)$_2$SOD and Ile137-Cu(II)$_2$Co(II)$_2$SOD. Signals are labelled according to the usually reported labelling of WT-Cu(II)$_2$Co(II)$_2$SOD hyperfine shifted signals

Signal	M δ (ppm)	WT δ (ppm)	Ile137 δ (ppm)	Assignment
A	63.3	66.0	63.3	His63 Hδ_2
B	57.1	56.4	57.3	His120 NHδ_2
C	49.7	50.3	48.4	His46 NHε_2
D	49.7	49.4	49.6	His71 Hδ_2
E	49.2	48.8	47.3	His80 Hδ_2
F	47.1	46.2	47.3	His80 HNε_2
G	39.3	40.9	47.3	His46 Hδ_2
K	39.3	34.6	38.6	His48 NHδ_1
I	35.6	36.3	36.1	Asp83 Hβ_1
H	35.6	38.5	43.8	His120 Hε_1
J′	35.6	35.8	36.1	Asp83 Hβ_2
J	35.6	35.6	36.1	His71 HNε_2
L	32.4	28.4	38.0	His48 Hδ_2
M	27.7	25.5	20.1	His46 Hε_1
N	24.2	23.6	23.7	His120 Hδ_2
O	23.6	19.6	22.5	His48 Hε_1
P	19.3	18.3	16.8	His46 Hβ_1
R	−3.9	−5.6	−8.1	His46 Hβ_2
Q	−6.3	−5.6	−6.5	His71 Hβ_2

The NOESY spectrum of the monomer is of poorer quality than for WT-Cu(II)$_2$Co(II)$_2$SOD, though recorded with a slightly longer experimental time. This is indicated, in the spectrum of M-Cu(II)Co(II)SOD derivative, by the absence of cross peaks between signal A and signals K and L, previously observed in the WT-Cu(II)$_2$Co(II)$_2$SOD (i.e., cross peaks 9 and 10, Fig. 6A). The decrease by a factor of two in τ_r (rotational correlation time) causes a decrease by a factor of two in the NOE intensity. For example, the extent of the one-dimensional NOE observed on signal C, when signal M is saturated at 200 MHz, is 2.8 ± 0.4% in the dimer and 1.0 ± 0.3% in the monomer. Since the T_1 values of signal C in the two derivatives are basically similar, the NOEs are consistent with a 50% reduction of the rotational correlation time. Again this effect provide spectroscopic evidence of the monomeric nature of the presently investigated derivative.

The occurrence of a sizable increase of the hyperfine shift of His48 imidazole ring protons is, perhaps, the most noteable feature of the ^{1}H NMR spectrum of M-Cu(II)Co(II)SOD. The same observation, though of different magnitude, was observed for the SOD analog

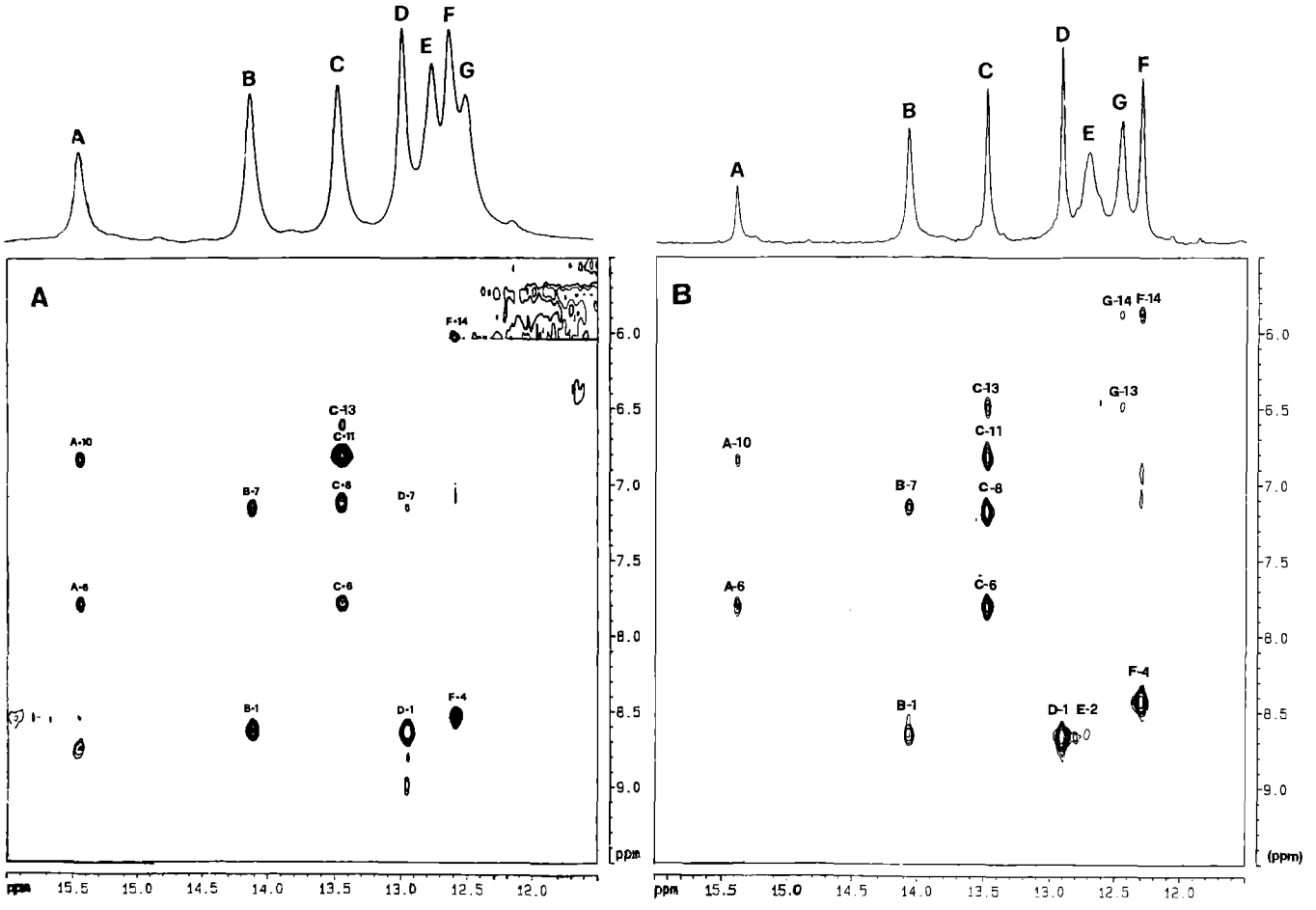

Fig. 8. 600 MHz ^{1}H NMR NOESY spectra of **A** WT-Cu(I)$_2$Zn(II)$_2$SOD and **B** M-Cu(I)Zn(II)SOD. Signals are labeled according to the labeling reported in Table 2. Conditions: mixing time 100 ms, relaxation delay 500 ms

Thr137Ile and was related to the occurrence of an increase in the Cu-N48 bond strength which makes the chromophore more axial (Bertini et al. 1989). The effect observed on the monomer as well as on the Ile137 mutated protein is opposite to that observed upon addition of anions like azide or cyanide (Banci et al. 1990d, 1989b; Bertini et al. 1991b) which cause a sizable decrease of the hyperfine shift of His48 proton resonances.

The assignments made here on the basis of the NOESY experiment in comparison with the NMR data on WT-Cu(II)$_2$Co(II)$_2$SOD is confirmed by the interaction of M-Cu(II)Co(II)SOD with sodium azide. The chemical shifts of the hyperfine shifted signals of M-Cu(II)Co(II)SOD with increasing amounts of sodium azide are displayed in Fig. 7. Because only signals of copper-coordinated residues are affected by interaction with azide, signals I, J, J', D, E are readily assigned to protons of cobalt-coordinated residues. Their shift is essentially unaltered with respect to WT-Cu(II)$_2$Co(II)$_2$SOD. With regard to signals of copper-coordinated residues, the well known chemical shift dependence of signals K, L, and O of WT-Cu(II)$_2$Co(II)$_2$SOD with azide concentration has been previously discussed. Signals deriving from His48 protons move toward the diamagnetic region, indicating that the quenching of the hyperfine coupling of His48 poton signals upon azide binding is observed in the case of the monomer derivative as well. The shift of the signal of the bridging His63 (A), as well as that of two of the three imidazole ring protons of His46, should experience an opposite trend, i.e. a chemical shift increase.

The affinity constant of M-Cu(II)Co(II)SOD for azide is $10.6 \pm 1.5\ M^{-1}$. Interestingly this value is lower than that measured for WT-Cu(II)$_2$Co(II)$_2$SOD ($138 \pm 5\ M^{-1}$) and correlates with a decrease in activity observed for the monomer. A similar trend of azide affinity and enzymatic activity has been found in most SOD analogs investigated to date (Beyer et al. 1987; Banci et al. 1988). This correlation demonstrates the importance of electrostatic factors in the catalytic reaction. For M-SOD the introduction of two negative charges (i.e. Glu), even if on the surface and far from the metal size, directly or indirectly modifies the electrostatic field around the protein, thus affecting the entrance of negative ions into the catalytic channel.

Cu(I)Zn(II)SOD derivatives. The reduced form of native SOD has been characterized through ^{1}H NMR spectroscopy (Lippard et al. 1987; Bertini et al. 1991a; Cass et al. 1977b; Stoesz et al. 1979; Mota de Freitas et al. 1990; Paci et al. 1990). A previous reported investigation of WT-Cu(I)$_2$Zn(II)$_2$SOD (Bertini et al. 1991a) has allowed the assignment of imidazole ring resonances of the dimeric enzyme. NOESY experiments on the reduced

Table 2. Chemical shift values of imidazole ring proton resonances of M-Cu(I)Zn(II)SOD and WT-$Cu(I)_2Zn(II)_2$SOD, at 298 K and pH 5.5. Signals are labelled according to the previously reported labelling of the imidazole ring proton resonances of WT-$Cu(I)_2Zn(II)_2$SOD (Bertini et al. 1991 a)

Signal	M δ (ppm)	WT δ (ppm)	Assignment
A	15.38	15.40	His71 HNε_2
B	14.06	14.06	His43 HNε_2
C	13.48	13.42	His46 HNε_2
D	12.90	12.90	His43 HNδ_1
E	12.69	12.70	His80 HNε_2
F	12.29	12.54	His48 HNδ_1
G	12.44	12.44	His63 HNε_2
1	8.64	8.64	His43 Hε_1
2	8.63	8.57	His80 Hε_1
3	–	8.54	His110 Hε_1
4	8.41	8.52	His48 Hε_1
5	–	8.29	His120 Hε_1
6	7.79	7.78	His71 Hε_1
7	7.14	7.14	His43 Hδ_2
8	7.11	7.11	His46 Hδ_2
9	6.91	6.86	His80 Hδ_2
10	6.84	6.82	His71 Hδ_2
11	6.78	6.78	His46 Hε_1
12	–	6.64	His120 Hδ_2
13	6.48	6.57	His63 Hε_1
14	5.86	6.05	His64 Hδ_2

monomeric derivative (Fig. 8 B) have been similarly performed and compared with the data obtained on the analogous dimeric wild type (Fig. 8 A). As above a sizable reduction in signal linewidth of the monomer is observed. This effect is most apparent in the region between 17 and 12 ppm, where well resolved NH resonances of imidazole ring protons are observed. The obvious comparison of the two spectra of Fig. 8 allows the assignment of signals, as reported in Table 2. For comparison the signals have been labeled as in a previous reported investigation of WT-$Cu(I)_2Zn(II)_2$SOD (Bertini et al. 1991 a). It is observed that while chemical shifts of the non-metal coordinated His43 resonances are identical, for other metal-coordinated residues some variations are observed. In particular, the two assigned signals of His48 (NHδ_1 and Hε_1) and two of the three imidazole ring resonance of His63 (Hε_1 and Hδ_2) experience decreases in chemical shifts from 0.09 to 0.25 ppm in the monomer with respect to the dimer, suggesting that the performed mutations reflect slight changes in the active site. Nevertheless the NOESY spectrum does not show evidence of significant changes in the interproton distances: all the observed connectivities of spectrum 8 A are confirmed in the monomer derivative, with relative intensities of cross peaks always conserved. The narrower signals afford additional interpretative information from bidimensional maps. For example, connectivities involving signals E and G in the monomer are visible in the NOESY spectrum, while in the dimer, connectivities G-13, G-14, E-2, could be detected only through monodimensional NOE difference spectra.

Concluding remarks

The spectroscopic characterization of a monomeric analog of SOD reveals some structural changes in the ligand arrangement around the metal ions: the increase in $A_{\parallel}$, the axial EPR spectrum, the increase in Cu–OH_2 distance, the ipsochromic shift of d-d transitions and some variations in the hyperfine shifts of the histidine protons in the axial EPR spectrum, the increase in Cu–OH_2 distance, the ipsochromic shift of d-d transitions and some variations in the hyperfine shifts of the histidine protons in M-Cu(II)Co(II)SOD indicate a structural change of the CuN_4 chromophore towards planarity. The above spectroscopic parameters are similar to those observed in the Thr137Ile SOD analog for which a slight distortion toward planarity (Banci et al. 1991 b) and a 1.4-fold reduction in specific activity (Bertini et al. 1989) (probably originating from changes in hydrophilicity (Bertini et al. 1989) and altered arrangement of charged residues in the active site channel (Banci et al. 1992)) were observed. The observation that substitution so far from the metal ions provides structural changes substantially analogous to those determined by the replacement of a residue inside the active cavity may shed new light in the understanding of the factors affecting structure-function relationships in SOD. In the monomer, substitutions so far from the metal ions (1.3 and 1.4 nm from copper(II) to Phe50 and Gly51) and from the active site channel would probably not *directly* induce a significant change in the active site. It seems more likely that such structural changes derive *indirectly* via extensive solvation of the newly exposed dimer interface and/or its distortion. It is possible that the similar arrangement around copper of Thr137Ile SOD and M-SOD is due to a balance of different contributions; the active channel is probably different since one is much more active than the other.

In M-SOD such changes presumably may also effect the active site channel which contributes to substrate docking and could be responsible for an approximately 10-fold reduction in specific activity observed in the monomer. In other mutated proteins such those in which the Arg143 (Beyer et al. 1987; Banci et al. 1988) has been substituted with a neutral or negative ligand or where Glu133 (Getzoff et al. 1992) has been replaced with a neutral residue, it has been shown that electrostatic forces are important in determining the dismutation rate under non saturating conditions. For monomeric SOD, reduced enzymatic activity may likely be ascribed to the introduction of two negative groups, though far from the active site, and/or to the restructuring of the exposed dimeric interface with concomitant shift of various unspecified charged residues. This hypothesis is consistent with the observed 15-fold reduction in affinity for azide.

Finally the monomerized protein, because of its reduced molecular weight, shows narrower NMR linewidths thus providing additional useful structural information. It would therefore also seem likely that larger proteins with higher quaternary structure (e.g., tetrameric human catalase) could be similarly "monomerized" by appropriate mutagenesis and thus permit for the first time NMR studies of large proteins not now accessible to this kind of analysis.

Acknowledgements. The Italian Council for Research (C.N.R.) is acknowledged for financial support to M.S.V. who prepared the mutated protein here described at Chiron Corporation, in 1990.

References

Banci L, Bertini I, Luchinat C, Monnanni R, Scozzafava A, Salvato B (1986) A spectroscopic investigation of Co_2Zn_2- and Co_2Co_2-superoxide dismutase. Gazz Chim Ital 116:51–54

Banci L, Bertini I, Luchinat C, Scozzafava A (1987) Nuclear relaxation in the magnetic coupled system Cu_2Co_2SOD. J Am Chem Soc 109:2328–2334

Banci L, Bertini I, Luchinat C, Hallewell RA (1988) An investigation of superoxide dismutase Lys-143, Ile-143, and Glu-143 mutants: Cu_2Co_2SOD derivatives. J Am Chem Soc 110:3629–3633

Banci L, Bertini I, Luchinat C, Piccioli M, Scozzafava A, Turano P (1989a) ^{1}H NOE studies on dicopper(II) dicobalt(II) superoxide dismutase. Inorg Chem 28:4650–4656

Banci L, Bertini I, Luchinat C, Piccioli M, Scozzafava A (1989b) Cyanide and azide behave in a similar fashion versus cupro-zinc superoxide dismutase. J Biol Chem 264:9742–9744

Banci L, Bertini I, Luchinat C, Piccioli M (1990a) Spectroscopic studies on Cu_2Zn_2SOD: a continous advancement of investigation tools. Coord Chem Rev 100:67–103

Banci L, Bertini I, Cabelli DE, Hallewell RA, Luchinat C, Viezzoli MS (1990b) Investigation of copper-zinc superoxide dismutase Ser-137 and Ala-137 mutants. Inorg Chem 29:2398–2403

Banci L, Bencini A, Bertini I, Luchinat C, Viezzoli MS (1990c) The angular overlap analysis of the spectroscopic parameters of copper-zinc SOD and its mutants. Gazz Chim Ital 120:179–185

Banci L, Bencini A, Bertini I, Luchinat C, Piccioli M (1990d) ^{1}H NOE and ligand field studies of superoxide dismutase with anions. Inorg Chem 29:4867–4873

Banci L, Bertini I, Cabelli DE, Hallewell RA, Tung JW, Viezzoli MS (1991a) A characterization of copper/zinc superoxide dismutase mutants at position 124-Zinc deficient proteins. Eur J Biochem 196:123–128

Banci L, Bertini I, Cabelli DE, Hallewel RA, Luchinat C, Viezzoli MS (1991b) Advances in understanding of the structure-function relationship in Cu, Zn superoxide dismutase. Free Rad Res Commun 12–13:239–251

Banci L, Bertini I, Luchinat C, Piccioli M (1991c) Frontiers in NMR of paramagnetic molecules: ^{1}H NOE and related experiments. In: NMR and Macromolecular Structure (Bertini I, Niccolai N and Molinari H, eds.) Ch. 2, VCH, Weinheim

Banci L, Carloni P, La Penna G, Orioli PL (1992) Molecular dynamics studies on superoxide dismutase and its mutants: the structural and functional role of Arg143. J Am Chem Soc 114: 6994–7001

Banci L, Bertini I, Luchinat C, Piccioli M, Scozzafava A (1993) 1D versus 2D ^{1}H NMR experiments in dicopper, dicobalt superoxide dismutase: a further mapping of the active site. Gazz Chim Ital 123:95–100

Bertini I, Luchinat C (1986) NMR of paramagnetic molecules in biological systems. Benjamin/Cummings, Menlo Park, CA

Bertini I, Scozzafava A (1981) Copper(II) as probe in substituted metalloproteins. In: Metal ions in biological systems, Vol 12. Siegel H (ed) Marcel Dekker, New York, pp 31–74

Bertini I, Lanini G, Luchinat C, Messori L, Monnanni R, Scozzafava A (1985a) An investigation of Cu_2Co_2SOD and its anion derivatives. J Am Chem Soc 107:4391–4396

Bertini I, Luchinat C, Mancini M, Spina G (1985b) The dipolar coupling between unpaired electrons and resonanting nuclei. In: Magneto-structrual correlations in exchanged coupled systems. Gatteschi D, Kahn O, Willett RD (eds) Reidel, Dordrecht, pp 421–461

Bertini I, Luchinat C, Viezzoli MS (1986) Metal substitution as a tool for the investigation of zinc proteins. In: Zinc enzymes. Bertini I, Luchinat C, Maret W, Zeppezauer M (eds) Birkhauser, Cambridge MA, pp 27–47

Bertini I, Banci L, Luchinat C, Bielski BHJ, Cabelli DE, Mullenbach GT, Hallewell RA (1989) An investigation of a human erythrocyte SOD modified at the position 137. Inorg Chem 111:714–719

Bertini I, Capozzi F, Luchinat C, Piccioli M, Viezzoli MS (1991a) Assignment of active site protons in the ^{1}H NMR spectrum of reduced human Cu, ZN superoxide dismutase. Eur J Biochem 197:691–697

Bertini I, Lepori A, Luchinat C, Turano P (1991b) Role of Arg-143 in human Cu_2Zn_2SOD studied through anion binding. Inorg Chem 30:3363–3364

Bertini I, Luchinat C, Piccioli M (1994) Copper zinc superoxide dismutase: a paramagnetic protein that provides a unique frame for the NMR investigations. Progr Nucl Magn Reson Spectrosc 26:91–140

Beyer WF, Fridovich I, Mullenbach GT, Hallewell RA (1987) Examination of the role of arginine-143 in the human copper and zinc superoxide dismutase by site-specific mutagenesis. J Biol Chem 262:11182–11187

Blackburn NJ, Hasnain SS, Binsted N, Diakun GP, Garner CD, Knowles PF (1984) An extended X-ray absorption fine-structure study of bovine superoxide dismutase in aqueous solution. Biochem J 219:985–990

Cass AEG, Hill HAO, Smith BE, Bannister JV, Bannister WH (1977a) Carbon-2 proton exchange at histidine-41 in bovine erythrocyte superoxide dismutase. Biochem J 165:587–589

Cass AEG, Hill HAO, Smith BE, Bannister JV, Bannister WH (1977b) Investigation of the structure of bovine erythrocyte superoxide dismutase by ^{1}H nuclear magnetic resonance spectroscopy. Biochemistry 16:3061–3066

Dugad LB, La Mar GN, Unger SW (1990) The influence of molecular correlation time on the homonuclear Overhauser effect in paramagnetic proteins. J Am Chem Soc 112:1386–1392

Ernst RR, Bodenhausen G, Wokaun A (1987) Principles of NMR in one and two dimensions. Clarendon Press, Oxford

Fee JA (1973) Studies on the reconstitution of bovine erythrocyte superoxide dismutase. IV: Preparation and some properties of the enzyme in which Co(II) is substituted by Zn(II). J Biol Chem 248:4229–4234

Forman JH, Evans HJ, Hill RL, Fridovich I (1973) Histidine at the active site of superoxide dismutase. Biochemistry 12:823–827

Fridovich I (1974) Superoxide dismutase. Adv Enzymol 41:35–97

Fridovich I (1987) Superoxide dismutase. Adv Enzymol Relat Areal Mol Biol 58:61–97

Getzoff ED, Cabelli DE, Fisher CL, Parge HE, Viezzoli MS, Banci L, Hallewell RA (1992) Faster superoxide dismutase mutants designed by enhancing electrostatic guidance. Nature 358:347–351

Inubushi T, Becker ED (1983) Efficient detection of paramagnetically shifted NMR resonances by optimizing the WEFT pulse sequence. J Magn Reson 512:128–133

Koenig SH, Brown RD III (1987) In: NMR spectroscopy of cells and organisms. Gupta RK (ed) CRC Press, Boca Raton, pp 75–85

Koenig SH, Brown RD III (1990) Field-cycling relaxometry of protein solutions and tissue. Implication for MRI. Progn Nucl Magn Reson Spectrosc 22:487–567

Lecomte JTJ, Unger SW, La Mar GN (1991) Practical considerations for the measurements of the mononuclear Overhauser effect on strongly relaxed protons in paramagnetic proteins. J Magn Reson 94:112–122

Lever ABP (1984) Inorganic electronic spectroscopy, 2nd edn. Elsevier, Amsterdam

Lippard SJ, Burger AR, Ugurbil K, Pantoliano MW, Valentine JS (1987) Nuclear magnetic resonance and chemical modification studies of bovine erythrocyte superoxide dismutase: evidence for zinc-promoted organization of the active site structure. Biochemistry 16:1136–1141

Marion D, Wutrich K (1983) Application of phase sensitive 2-dimensional correlated spectroscopy (COSY) for measurements of ^{1}H-^{1}H spin-spin constants in proteins. Biochem Biophys Res Commun 113:967–974

McCord JM, Fridovich I (1969) Superoxide dismutase. An enzymatic function for erythrocuprein (hemocuprein) J Biol Chem 244: 6049–6055

Mota de Freitas D, Ming L-J, Ramasamy R, Valentine JS (1990) ^{35}Cl and ^{1}H NMR study of anion binding to reduced bovine copper-zinc superoxide dismutase. Inorg Chem 29:3512–3518

Paci M, Desideri A, Sette M, Ciriolo MR, Rotilio G (1990) Assignment of imidazole resonances from two-dimensional proton NMR spectra of bovine Cu, Zn superoxide dismutase. Evidence for similar active site conformation in the oxidized and reduced enzyme. FEBS Lett 263:127–130

Pantoliano MW, Valentine JS, Mammone RJ, Scholler DM (1979) Reversible loss of metal ions from the zinc binding site of copper-zinc superoxide dismutase. The low pH transition. J Am Chem Soc 101:6454–6456

Pantoliano MW, Valentine JS, Nafie LA (1982) Spectroscopic studies of copper(II) bound at the native copper site or substituted at the native zinc site of bovine erythrocuprein (superoxide dismutase). J Am Chem Soc 104:6310–6317

Rotilio G, Morpurgo L, Giovagnoli C, Calabrese L, Mondovì B (1972a) Metal sites of copper proteins. III. Simmetry of copper in bovine superoxide dismutase and its function significance. Biochemistry 11:2187–2192

Rotilio G, Calabrese L, Bossa F, Barra D, Finazzi Agró A, Mondovì B (1972b) Properties of the apoprotein and role of copper and zinc in protein conformation and enzyme activity of bovine superoxide dismutase. Biochemistry 11:2182–2187

Sklenar V, Bax A (1987) Spin-echo water suppression for the generation of pure-phase two dimensional NMR spectra. J Magn Reson 74:469–479

Stoesz JD, Malinowski DP, Redfield AG (1979) Nuclear magnetic resonance study of solvent exchange and nuclear Overhauser effect of the histidine protons of bovine superoxide dismutase. Biochemistry 18:4669–4675

Tainer JA, Getzoff ED, Beem KM, Richardson JS, Richardson DC (1982) Determination and analysis of the 2-Å structure of copper, zinc superoxide dismutase. J Mol Biol 160:181–217

Valentine JS, Pantoliano MW (1982) Protein-metal ion interaction in cuprozinc protein (superoxide dismutase). In: Copper proteins, Vol 3. Spiro G (ed). Wiley, New York, pp 291–358